Kinetic Study of the Hexacyanoferrate (III) Oxidation of Dihydroxyfumaric Acid in Acid Media

B. García,* R. Ruiz, and J. M. Leal

Universidad de Burgos, Departamento de Química, 09001 Burgos, Spain

Received: January 9, 2008; Revised Manuscript Received: February 21, 2008

The kinetics of the hexacyanoferrate (III) oxidation of dihydroxyfumaric acid to hexacyanoferrate (II) and diketosuccinic acid was looked into within the 0.04 to 5.3 M HCl acidity range under different temperatures, ionic strengths, and solvent permittivity conditions. The kinetic effect of alkali metal ions, transition metal impurities, and substrate concentrations have also been analyzed. The observed inhibition effect brought about by addition of the reaction product, hexacyanoferrate (II), is a sign of a complex mechanism. The rate constants remained essentially unchanged up to 1 M HCl, diminished between 1.0 and 3.0 M HCl, and rose above 3.0 M HCl. Depending on the medium acidity, three mechanisms can be put forward, which involve different kinetically active forms. At low acidity, the rate-determining step involves a radical cation and both the neutral and the anion substrate forms are equally reactive ($k_1 = k_2 = 2.18 \pm 0.05$ M^{-1} s^{-1}, $k_{-1} = 0.2 \pm 0.03$). When the medium acidity is boosted, the rate-determining step involves the neutral dihydroxyfumaric acid and two hexacyanoferrate (III) forms. In the intermediate region the rate constant diminished with rising $[H^+]$ ($k'_1 = 0.141 \pm 0.01$ and $k'_2 = 6.80 \pm 0.05$). Specific catalytic effect by binding of alkali metal ions to oxidant has not been observed. In all instances it was assessed that the substrate decomposition is slow compared to the redox reaction.

Introduction

Dihydroxyfumaric acid (HADF) is an efficient reductant compound in a number of applications, and has been suggested as an intermediate species in the biosynthesis of sugars, uronic acids, and vitamin C.[1] HADF serves to improve wine quality by enlarging its aging and stability. Added to only small amounts (1−10 mM), it improves the wine taste and flavor, leaving out turbidity and inhibiting catechol and phenol oxidation.[2] HADF often is used as a disinfectant in contact lenses, hydrophilic plastic materials,[3] and wastewater,[4] and as color destabilizing in cleaning products.[5] Maleic acids and the HADF o-acetylderivatives are used as analgesic and antipyretic drugs.[6]

X-ray diffraction measurements of solid samples support the trans conformation;[7] comparison with the dissociation constants of maleic (cis) and fumaric (trans) acids indicate that also in solution the trans conformation dominates.[8] In acidic and basic solutions it undergoes the keto−enol equilibrium characteristic of β-ketoacids, responsible for the decarboxylation of HADF.[1,9–12] So far, very little has been published on the oxidation kinetics of HADF; the kinetics is first order both in reactant and substrate species.[13] HADF is prone to undergo two successive acid−base equilibria ($pK_1 = 1.57$ and $pK_2 = 3.36$)[8] according to

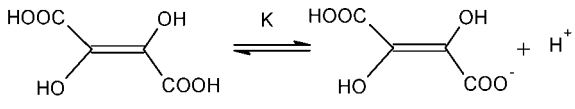

(1)

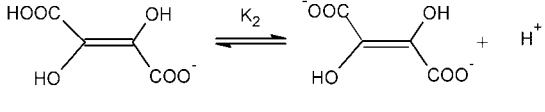

(2)

In this work, a thorough study of the hexacyanoferrate (III) oxidation of HADF in the 0.04−5.3 M HCl acidity range has been undertaken. Although a relatively poor oxidant, hexacyanoferrate (III) (also known as ferricyanide) is a selective outer-sphere reactant applicable to the most easily oxidizable substrates, and it is frequently used as an interceptor of free radicals; this feature turns this species into an efficient one-electron oxidant particularly interesting in the comparative study of octahedral complexes. In alkaline media, a large number of oxidations have been carried out, the mechanisms being dependent on the particular substrate and the catalyst used.[14–24] Although the oxidizing ability enhances in acidic solvents, only few contributions have been published in such media.[14] In acidic micelar media (sodium dioctylsulfosuccinate) the oxidation of cysteine is first-order in oxidant and reductant.[25]

Hexacyanoferrate (III) may undergo three acid−base equilibria,[14] according to

$$H_3Fe(CN)_6 \overset{K_3}{\rightleftharpoons} H_2Fe(CN)_6^- + H^+ \quad (3)$$

$$H_2Fe(CN)_6^- \overset{K_4}{\rightleftharpoons} HFe(CN)_6^{2-} + H^+ \quad (4)$$

$$HFe(CN)_6^{2-} \overset{K_5}{\rightleftharpoons} Fe(CN)_6^{3-} + H^+ \quad (5)$$

with ionization constants $pK_3 = -6.25$, $pK_4 = -3.23$, and $pK_5 = -0.6$. Hexacyanoferrate (II) (ferrocyanide) may, in turn, undergo four acid−base equilibria:

$$H_4Fe(CN)_6 \overset{K_6}{\rightleftharpoons} H_3Fe(CN)_6^- + H^+ \quad (6)$$

$$H_3Fe(CN)_6^- \overset{K_7}{\rightleftharpoons} H_2Fe(CN)_6^{2-} + H^+ \quad (7)$$

$$H_2Fe(CN)_6^{2-} \overset{K_8}{\rightleftharpoons} HFe(CN)_6^{3-} + H^+ \quad (8)$$

$$HFe(CN)_6^{3-} \overset{K_9}{\rightleftharpoons} Fe(CN)_6^{4-} + H^+ \quad (9)$$

with $pK_6 = -2.54$, $pK_7 = -1.08$, $pK_8 = 2.65$, and $pK_9 = 4.19$.[14]

* Corresponding author. E-mail: begar@ubu.es.

10.1021/jp800208s CCC: $40.75
Published on Web 05/13/2008

TABLE 1: $[Fe(CN)_6]K_3$ Absorptivities (ϵ, $M^{-1}cm^{-1}$) at Different Wavelengths and HCl Concentrations

$[H^+]$, M	ε_{416}	ε_{320}	ε_{300}	ε_{260}
0.01	1015	1174	1620	1270
0.10	1013	1171	1622	1263
1.00	1020	1180	1677	1250
2.00	1027	1171	1642	1221
3.00	1035	1167	1629	1198
4.00	1047	1170	1632	1166

Experimental Section

The absorption measurements were performed on a diode array spectrophotometer set up with a Peltier accessory to control temperature. To leave out any HADF decomposition effect on the oxidation kinetics, freshly prepared solutions were always used. The oxidation rate constants were deduced from evaluation of the course of the reaction by monitoring under pseudo first-order conditions (an excess of HADF) the disappearance of the oxidant species at $\lambda = 416$ nm. The absorbance-time data-pairs were fitted to the kinetic equation

$$A = (A_0 - A_\infty)e^{-k_{obs}t} + A_\infty \qquad (10)$$

The experiments were carried out at 25 ± 0.1 °C throughout, if not indicated otherwise, using HCl to attain the proper acidity level. The involvement of radical species was assessed by the polymerization test: 2 mL of freshly distilled acrylonitrile was added in an inert nitrogen atmosphere to a 20 mL sample of the reacting mixture containing ferricyanide (0.05 M), HADF (0.05 M), and HCl (0.1 M), with the result of progressive formation of a white solid across the whole solution. When the experiment was repeated in the absence of HADF using the same conditions, the test became negative; however, when the test was repeated excluding the oxidant, the test became positive and the reaction was slowed down as a result of the HADF decarboxylation.

Results and Discusion

1. Kinetics of the HADF Decarboxylation. The kinetics of the HADF decarboxylation to glycolaldehyde in acidic medium involves a two-step mechanism.[26,27] Combination of mass spectrometry measurements and computational chemistry calculations has shown that the dissociative ionization generates the hydrogen-bridged radical cation $[H_2O\cdots HCO_2H]^{\bullet+}$.[28] Mass spectrometry measurements reveal that transfer of the 1,5 hydrogen atoms and the sequential release of CO lead to such a hydrogen-bridged product. The unimolecular metastable dissociation of $[H_2O\cdots HCO_2H]^{\bullet+}$ leads to the proton-bound ion $[H_2O\cdots HOCO]^+$ and to a hydronium ion. The decomposition rate constants of HADF as well as the keto−enol equilibrium constants have been evaluated at acidity levels of 1 to 10^{-4} M sulfuric acid, the reaction being first-order in HADF.[10–12,29] In this work, the decarboxylation of HADF has been looked into over the 0.01 to 1.0 M HCl range. The reaction fits well to a first-order kinetics according to eq 10; the rate constants remain unchanged ($k_{obs} = 4.6 \times 10^{-4} \pm 6 \times 10^{-5}$ s^{-1}), whereas at 0.01 M the values dropped ($2.7 \times 10^{-4} \pm 4 \times 10^{-5}$ s^{-1}), in fairly good agreement with those deduced in sulfuric acid.[10]

2. Kinetics of the HADF Hexacyanoferrate (III) Oxidation. ***(a) Fulfillment of the Lambert−Beer Law for [Fe(CN)$_6^{3-}$].*** The monitoring species, $[Fe(CN)_6^{3-}]$, was assessed to fulfill the Lambert−Beer law within the 0.01−4.0 M HCl acidity range. Table 1 lists the absorptivity coefficients, ϵ, measured at different wavelengths. The ϵ values remained essentially constant with medium acidity except at $\lambda = 260$ nm, where they diminished slightly. This feature indicates that all kinetically active oxidant forms display absorption at the 416 nm wavelength selected, and reveals that any potential spectrophotometric distinction between the different protonated forms is unlikely.[30] Regarding the reaction product, hexacyanoferrate (II), the absorption maximum is located at 220 nm, and neither of its protonated forms show any spectral interference with the reactant species.[31]

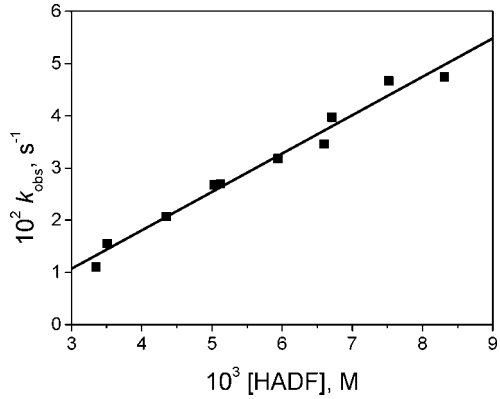

Figure 1. k_{obs} vs substrate concentration [HADF] plot; $[Fe(CN)_6^{3-}] = 5 \times 10^{-4}$ M, [HCl] = 1.0 M, $T = 25$ °C.

TABLE 2: k_{obs} Values at Different $[Fe(CN)_6^{3-}]$ Concentrations ([HCl] = 1.0 M, [HADF] = 5×10^{-3} M, T = 25 °C)

10^4 $[Fe(CN)_6^{3-}]$, M	10^2 (k_{obs}), s^{-1}
1.67	2.90 ± 0.06
2.50	2.81 ± 0.04
3.33	2.69 ± 0.06
4.17	2.52 ± 0.04
5.00	2.44 ± 0.05
5.83	2.40 ± 0.04

(b) Effect of the Initial Substrate Concentration. The kinetic runs were monitored using HADF concentration in excess. Figure 1 shows the variation of k_{obs} versus the substrate concentration; the data-pairs fit fairly well to the equation: $k_{obs} = -0.0076\ (\pm 0.0012) + 6.7242\ (\pm 0.3015)$ [HADF]. The rather small intercept obtained bears out a kinetic first order in the substrate concentration.

(c) Effect of the Initial Oxidant Concentration. Table 2 shows the variation of k_{obs} with hexacyanoferrate (III). The data-pairs did not fit fairly well to eq 10. The kinetic order differed from unity, as shown by the soft progressive fall of the k_{obs} values when the oxidant concentration is boosted. This behavior is justified below.

2.1. Initial Rates. ***(a) Inhibition Effect by Hexacyanoferrate (II).*** When the hexacyanoferrate (III) reaction order in the oxidation of organic substrates is unity or close to unity both in oxidant and reductant species, the rate-determining step is the transfer of one electron from the substrate to the oxidant to produce hexacyanoferrate (II). When the product inhibits the overall reaction (Table 1, Supporting Information), this step becomes irreversible;[14] hence, the mechanism suggested at 1.0 M HCl involves the following steps:

$$Fe(CN)_6^{3-} + HADF \underset{k_{-1}}{\overset{k_1}{\rightleftharpoons}} Fe(CN)_6^{4-} + HADF^{\bullet+} \quad (11)$$

$$Fe(CN)_6 + HADF^{\bullet+} \xrightarrow{k_2} Fe(CN)_6^{4-} + P + 2H^+ \quad (12)$$

The formation of free radicals has been assessed by the initial polymerization test. The results deduced show that the test was negative in the absence of HADF and positive in the presence of HADF; the overall reaction became strikingly faster when HADF was present concurrently with hexacyanoferrate (III), compared to HADF alone in solution. These results denote that HADF is capable of generating free radicals, either through oxidation or in a much slower way through decarboxylation. The mechanism put forward resembles that of endiols such as 2,3-dihydroxy-2-propenal or ascorbic acid; however, in the latter cases, the initial step is irreversible. The hydroxyfumarate radical species bears similarity with the ascorbate radical suggested in the oxidation of ascorbic acid.[32–38] The product P (eq 12) would be the corresponding diketone, that is, diketosuccinic acid, as occurs in electrochemical oxidations[10,39] or by 2,6-dichlorophenolindophenol.[13] The rate equation applicable to this scheme leads to

$$-\frac{d[Fe(CN)_6^{3-}]}{dt} = \frac{2k_1k_2[HADF] \cdot [Fe(CN)_6^{3-}]^2}{k_2[Fe(CN)_6^{3-}] + k_{-1}[Fe(CN)_6^{4-}]} \quad (13)$$

Equation 13 accounts for the observed deviation from the first-order behavior quoted above (Table 2). In the initial stages, when $k_2\,[Fe(CN)_6^{3-}] \gg k_{-1}\,[Fe(CN)_6^{4-}]$, it is eq 14 that governs the overall reaction:

$$-\frac{d[Fe(CN)_6^{3-}]}{dt} = 2k_1[HADF][Fe(CN)_6^{3-}] \quad (14)$$

Therefore, we had to fall back on the initial-rate method, a time range where the product concentration is negligible. To study the product concentration effect on the reaction rate, hexacyanoferrate (II) was added to a particular amount of the reaction mixture; hence, eq 13 turns into eq 15:

$$r_0 = \frac{a}{b + k_{-1}[Fe(CN)_6^{4-}]_0} \quad (15)$$

with a and b being constant. The addition of ferrocyanide inhibits the overall reaction, the $1/r_0$ versus $[Fe(CN)_6^{4-}]$ plot leads to a

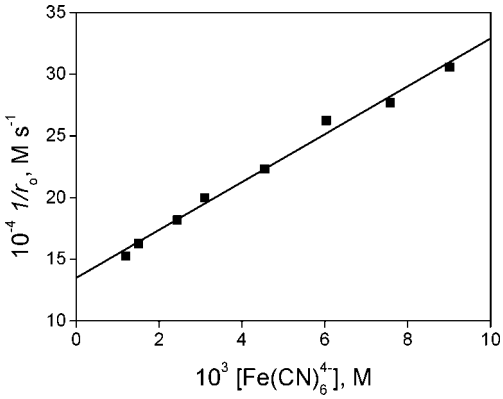

Figure 2. Reciprocal initial rate, $1/r_0$, as a function of the initial $[Fe(CN)_6^{4-}]$. $[H^+] = 1.0$ M, $[HADF] = 5 \times 10^{-3}$ M, $[Fe(CN)_6^{3-}] = 5 \times 10^{-4}$ M, $T = 25$ °C.

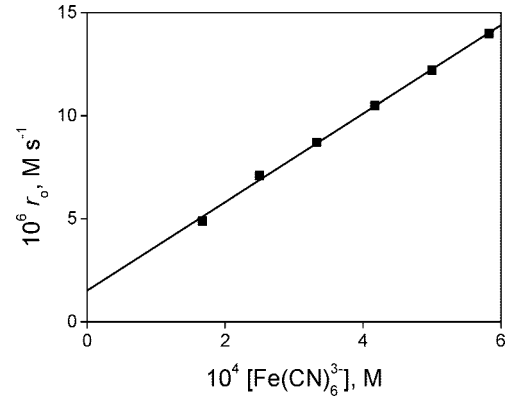

Figure 3. Initial Rate, r_0, as a function of the initial oxidant concentration. [HCl] = 1.0 M, [HADF] = 5×10^{-3} M, $T = 25$ °C.

fairly straight line ($r^2 = 0.998$) (Figure 2); the fitting of data yields the parameters $b/a = 1.35 \times 10^5$ and $a = 1.94 \times 10^7$.

(b) Effect of the Initial Oxidant Concentration. Figure 3 shows the variation of the initial rate with the oxidant concentration, the data fitting (Table 2, Supporting Information) leading to $r_0 = (1.365 \times 10^{-6} \pm 1.887 \times 10^{-7}) + (0.021815 \pm 4.96 \times 10^{-4})[Fe(CN)_6^{3-}]$, yielding the parameters $k_1 = 2.18 \pm 0.05$ M^{-1} s^{-1}, and from $b/a = 1.35 \times 10^5$ and $a = 1.94 \times 10^7$ determined above, we obtained $k_{-1}/k_2 = 0.092$, ($r^2 > 0.998$).

(c) The Ionic Strength Effect, XCl ($X^+ = Li^+, Na^+, K^+$). Table 3 lists the results of the experiments performed at two different acidity levels, 0.10 and 2.0 M HCl, varying the ionic strength by use of LiCl, NaCl, and KCl in the 0−0.5 M range. The data of Table 3A, with HCl = 0.1 M, show a soft decrease in rate when the ionic strength is boosted. The substrate concentration is split into the neutral form, HADF (predominant), and the monoanion form, ADF^- (eq 1), whereas the oxidant only adopts the $[Fe(CN)_6^{3-}]$ form. At 2.0 M acidity level, it is assumed that rate constants remain unchanged (Table 3B); in this case, the substrate is fully in the neutral form, whereas the oxidant is split into the equilibrium $[Fe(CN)_6^{3-}]$ and $[HFe(CN)_6^{2-}]$ (eq 5).

The observed fall in rate with rising ionic strength at 0.1 M HCl (Table 3A) cannot be accounted for by a simple primary salt effect, which would involve the neutral or the mono anion substrate forms. The secondary salt effect on the substrate acid−base equilibrium should also be ruled out because the equilibrium constant becomes unaffected by the medium acidity within the 0.04−1.00 M HCl range.

A third possible route should also be brought up here, due to the ion association effect set up between the anion oxidant form and the alkali-metal ion, by virtue of the following equilibria:[40]

$$Fe(CN)_6^{3-} + X^+ \overset{K_{XFe(III)}}{\rightleftharpoons} XFe(CN)_6^{2-} \quad (16)$$

$$Fe(CN)_6^{4-} + X^+ \overset{K_{XFe(II)}}{\rightleftharpoons} XFe(CN)_6^{3-} \quad (17)$$

In the present case it should not be inferred that such an effect is present, as deduced from the k_{obs} values (Table 3); the data listed show no unambiguous sequence to deduce specific catalysis. Bearing in mind that the reaction product, ferrocyanide, may bind up to two alkali cations, whereas the reactant, ferricyanide, may bind only one, the reversible step 11 along with the observed slightly negative catalytic effect could well account for the observed

TABLE 3: k_{obs} Values as a Function of the Ionic Strength, I, using XCl as a Neutral Salt: (a) LiCl, (b) NaCl, (c)KCl[a]

XCl, M	I, M	(a) 10^2 (k_{obs} ± error), s^{-1}	(b) 10^2 (k_{obs} ± error), s^{-1}	(c) 10^2 (k_{obs} ± error), s^{-1}
		(A) [HCl] = 0.1 M		
0.0	0.1	2.867 ± 0.064	2.978 ± 0.082	2.631 ± 0.038
0.1	0.2	2.268 ± 0.049	2.341 ± 0.058	2.222 ± 0.046
0.2	0.3	2.159 ± 0.047	2.114 ± 0.040	2.024 ± 0.044
0.3	0.4	2.044 ± 0.039	1.790 ± 0.032	1.971 ± 0.044
0.4	0.5	2.002 ± 0.044	1.762 ± 0.031	1.829 ± 0.036
0.5	0.6	1.914 ± 0.037	1.624 ± 0.030	1.788 ± 0.036
		(B) [HCl] = 2.0 M		
0.0	2.0	2.31 ± 0.01	2.23 ± 0.01	2.48 ± 0.02
0.1	2.1	2.26 ± 0.01	2.16 ± 0.02	2.31 ± 0.02
0.2	2.2	2.20 ± 0.01	2.11 ± 0.01	2.43 ± 0.02
0.3	2.3	2.33 ± 0.02	2.12 ± 0.01	2.49 ± 0.01
0.4	2.4	2.19 ± 0.01	2.05 ± 0.02	2.44 ± 0.01
0.5	2.5	2.21 ± 0.01	2.21 ± 0.01	2.30 ± 0.01

[a] [HCl] = 0.1 M, [HADF] = 5×10^{-3} M, [$Fe(CN)_6^{3-}$] = 5×10^{-4} M, T = 25 °C.

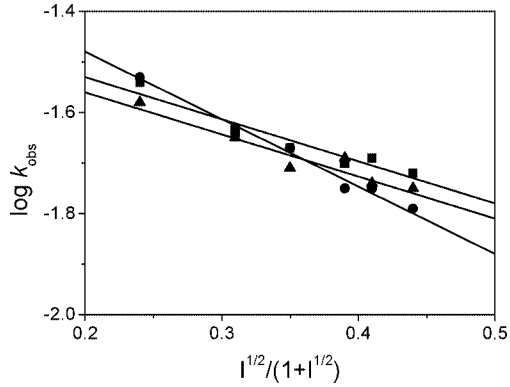

Figure 4. log k_{obs} vs ionic strength function $I^{1/2} + (1 + I^{1/2})$ plot. (●) LiCl, (■) NaCl and (▲) KCl. [HCl] = 0.1 M.

behavior; however, this effect would be small, because the alkali cation (X^+) effect on the reaction rate is small.

Figure 4 shows the fulfilment of eq 1 in the Supporting Information. The slopes deduced with all three cations used are small and close to 1.2, which supports the assumption that the rate-determining step involves charged species of different sign. In view that the oxidant charge is −3, that of the substrate should be a positive uninteger, consistent with the radical species assumed (eqs 11 and 12).

When the medium acidity is boosted to 2.0 M, the rate constant remains unchanged upon varying the ionic strength (Table 3B). At this acidity level the oxidant species is present in two different forms in equilibrium, [$Fe(CN)_6^{3-}$] and [$HFe(CN)_6^{2-}$],[14] whereas the only active substrate form in the rate-determining step is the neutral one. In the oxidation of ascorbic acid at [H^+] = 2.0 M, the entering protons are able to remove the alkali-metal ions from the hexahedral hexacyanoferrate (III) complex as a consequence of the protonation,[40] which justifies the nondependence on the nature of the particular salt used to adjust the ionic strength.

(d) Effect of Trace Metal Ions. Certain ion species present as impurities in the reaction medium may oxidize HADF;[41,42] hence, a set of experiments was carried out by adding variable initial amounts of the metal ions Cu(II) and Fe(III). Table 4 lists the k_{obs} values deduced, showing only an inappreciable effect. Likewise, in order to disguise the effect of any potential trace metal present in solution, an experiment was performed under the same conditions, this time adding EDTA (5×10^{-6} M) to the reacting mixture, giving rise to no noticeable difference in rate compared to the experiments in the absence of EDTA. It can then be concluded that the trace metal ions exert no noticeable effect as potential catalysts in the oxidation of HADF.

TABLE 4: k_{obs} as a Function of the Initial Impurity Concentration X^{n+}: (a) Fe^{3+}, (b) Cu^{2+} [a]

10^6 X^{n+} M	(a)10^2 (k_{obs} ± e)[b] s^{-1}	(b)10^2 (k_{obs} ± e)[b] s^{-1}
1	2.91 ± 0.03	3.05 ± 0.02
2	3.39 ± 0.02	3.15 ± 0.02
3	3.47 ± 0.03	3.27 ± 0.02
4	3.36 ± 0.03	3.06 ± 0.03
5	4.40 ± 0.05	2.80 ± 0.04
6	3.77 ± 0.04	2.67 ± 0.05

[a] [HCl] = 1.0 M, [HADF] = 5×10^{-3} M, [Fe(CN)63−] = 5×10^{-4} M, T = 25 °C. [b] e = error.

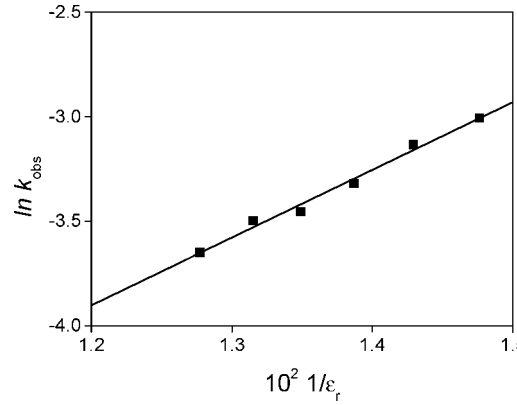

Figure 5. ln k_{obs} values as a function of the reciprocal solvent permittivity, $1/\varepsilon_r$. [HCl] = 1.0 M, [HADF] = 5×10^{-3} M, [$Fe(CN)_6^{3-}$] = 5×10^{-4} M, T = 25 °C.

(e) Solvent Permittivity Effect. The solvent permittivity was varied by use of water/ethanol mixtures. Table 3 in the Supporting Information shows the rise in rate when the solvent permittivity drops. The ln k_{obs} versus $1/\varepsilon_r$ plot leads to a straight line with positive slope ($r^2 > 0.995$) (Figure 5). For reactions between two ion species, the ln k versus $1/\varepsilon_r$ dependence is as follows:[43]

$$\ln k_{obs} = \ln k_{\infty} - \frac{N z_A z_B e^2}{4\pi\varepsilon_0 \varepsilon_r R T r_{\neq}} \qquad (18)$$

where k_∞ is the constant in the infinite dilution reference state. From the intercept, the $k_\infty = 4 \times 10^{-4}$ s^{-1} value was deduced.

(f) The Temperature Effect. A set of experiments was performed at different temperatures between 21.4 and 37.4 °C and three HCl concentrations (Table 5). The activation energies E_a, and the activation parameters enthalpy $\Delta H_0^{\ddagger}$ and entropy $\Delta S_0^{\ddagger}$ were calculated by least-squares fitting of the k_{obs} values at

TABLE 5: k_{obs} Values as a Function of Temperature[a]

T, °C	(a) $10^2(k_{obs} \pm$ error), s^{-1}	(b) $10^2(k_{obs} \pm$ error), s^{-1}	(c) $10^2(k_{obs} \pm$ error), s^{-1}	(d) $10^2(k_{obs} \pm$ error), s^{-1}
21.4	3.032 ± 0.050	2.478 ± 0.012	1.440 ± 0.069	2.120 ± 0.014
23.4	3.305 ± 0.065	2.713 ± 0.012	1.506 ± 0.011	2.435 ± 0.018
25.4	3.252 ± 0.066	2.942 ± 0.014	1.650 ± 0.070	2.542 ± 0.017
27.4	3.339 ± 0.059	3.309 ± 0.019	1.829 ± 0.070	2.788 ± 0.018
29.4	3.189 ± 0.079	3.523 ± 0.020	2.081 ± 0.080	3.180 ± 0.024
31.4	3.272 ± 0.060	3.792 ± 0.036	2.217 ± 0.090	3.688 ± 0.033
33.4	3.115 ± 0.076	4.064 ± 0.043	2.543 ± 0.021	4.298 ± 0.057
35.4		4.382 ± 0.063	2.812 ± 0.030	4.342 ± 0.016
37.4			3.303 ± 0.038	

[a] [HCl] = (a) 0.1 M; (b) 1.5 M; (c) 3.0 M; (d) 4.5 M. [HADF] = 5×10^{-3} M, $[Fe(CN)_6^{3-}] = 5 \times 10^{-4}$ M.

TABLE 6: Activation Energy, E_a, Frequency factor, A, Enthalpy, $\Delta H_0^{\ddagger}$ and Entropy, $\Delta S_0^{\ddagger}$

HCl, M	($E_a \pm$ error), kJ mol^{-1}	10^{-4} A, s^{-1}	$\Delta H^{\ddagger}$, kJ mol^{-1}	$\Delta S^{\ddagger}$, J K^{-1} mol^{-1}
0.10				
1.50	7.61 ± 0.23	1.11	6.91 ± 0.24	−42.38 ± 0.80
3.00	9.03 ± 0.49	6.80	8.92 ± 0.50	−36.78 ± 1.65
4.50	9.56 ± 0.67	26.00	8.97 ± 0.67	−35.77 ± 2.24

different temperatures (eq 19 and Table 6) to the transition-state equation:

$$\ln(k_{obs}/T) = (\ln k_B/h + \Delta S_0/R) - (\Delta H_0/R) \cdot (1/T) \quad (19)$$

where k_B and h are universal constants.

The Arrhenius and transition-state equations are not fully accomplished at HCl = 0.1 M. At this acidity level the reaction rate remains unaffected by the temperature increase. The modest frequency factor obtained, 10^4, is in line with reactions controlled by electrostatic forces between species oppositely charged.[44]

(g) The Medium Acidity Effect. Figure 6 shows the variation of the rate constants at different acidity levels in the 0.04−5.33 M HCl range. Three different acidity regions can be distinguished: Region I, 0.04−1.00 M HCl, the rate constant remains essentially constant within the margin of error; Region II, between 1.3 and 3.0 M HCl, the rate constants fall when the medium acidity is boosted; Region III, 3.0 M HCl and above, the rate constants rise when the medium acidity is raised. Above 5.3 M HCl, the reaction rate is too fast to be monitored by the techniques used. The oxidant and substrate reactive forms in each region can be discriminated on the basis of equilibria 1 to 9 and their corresponding constants. In Region I, $[H^+] < 1$ M, the oxidant species is predominantly in the $[Fe(CN)_6^{3-}]$ form, and the reaction product is in the $[H_2Fe(CN)_6^{2-}]$ form. Regarding the substrate, both the neutral and the anion forms are present concurrently. The observed nondependence of the reaction rate with the medium acidity gives away that the two forms react with similar rates through a complex scheme. At $[H^+] > 1$ M, the variation of k_{obs} with the medium acidity displayed two well-defined regions (2 and 3). Three different oxidant species must be taken into consideration: the nonprotonated, the monoprotonated, and the diprotonated ferricyanide ions, HADF being always in the neutral form. In Region II, a decrease in k_{obs} with increasing acidity is observed. Above 3.0 M (Region III), the k_{obs} values rose with the increase in medium acidity, according to a complex function.

(h) Stoichiometry. The reaction stoichiometry was determined by measuring the oxidant concentration remaining after completion of a kinetic run with the oxidant in excess. The 2:1 ratio found with other endiols such as 2,3-dihydroxy-2-propenal,[3] or ascorbic acid,[33−38] was not found here, but rather the [Ferricyanide]$_{completed}$/[HADF]$_{initial}$ ratio determined at three acidity levels, $[H^+]$ = 0.1, 1.0, and 2.0 M, was always 1.4:1. This feature should not be set down to interference of any HADF decarboxylation over the time needed to complete the redox reaction, because decarboxylation is 2 orders of magnitude slower. A 10-fold increase in the oxidant concentration results in a 1.60:1 oxidant/substrate ratio. These findings concur with a complex reaction, and the probable recombination of the hydroxyfumarate radicals in a diffusion-controlled step (forming HADF and diketosuccinic acid (P)) should be considered.

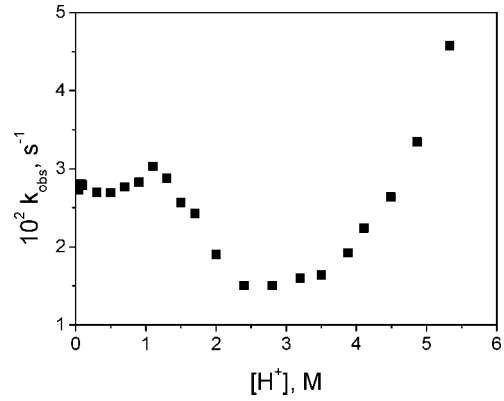

Figure 6. k_{obs} values as a function of medium acidity. [HADF] = 5×10^{-3} M, $[Fe(CN)_6^{3-}] = 5 \times 10^{-4}$ M, T = 25 °C.

3. Discussion

The kinetic data measured show that the overall reaction is prone to different schemes, depending on the acidity range. The mechanisms can be rationalized on the basis of the protonation extent of the reactant species, as well as that of hexacyanoferrate (II), whose inhibiting effect gives away its involvement as a reactive species. Unlike the ascorbic acid oxidation, where two k_{obs} stretches could be differentiated over the acidity range,[40] three regions can, in turn, be distinguished for HADF: in the first region, k_{obs} did not change appreciably with medium acidity, in the second region k_{obs} diminished with medium acidity, and in the third region k_{obs} increased.

Region I: $[H^+] < 1$ M. In this region, the rate constants can be regarded as being independent of medium acidity (Figure 6). The variation of k_{obs} with ionic strength (Table 3) and solvent permittivity (Figure 5) reveals a reaction mechanism that involves some cationic oxidant forms in the rate-determining step. At $[H^+] = 0.1$ M, the rate constants showed no temperature dependence (Table 5). In view of the substrate acid dissociation constant ($pK_1 = 1.57$), the neutral and the monoanion forms undergo equilibrium 1. Likewise, hexacyanoferrate (III) ($pK_5 = -0.6$, eq 5) is fully in the nonprotonated form, whereas hexacyanoferrate (II) is primarily diprotonated ($pK_8 = 2.65$)

(eqs 8 and 9). Hence, in addition to eqs 1, 8, and 9, the oxidation mechanism consists of the following reactions:

$$Fe(CN)_6^{3-} + HADF \xrightarrow{k_1} Fe(CN)_6^{4-} + HADF^{\bullet+} \quad (20)$$

$$H_2Fe(CN)_6^{2-} + HADF^{\bullet+} \xrightarrow{k_{-1}} Fe(CN)_6^{3-} + HADF + 2H^+ \quad (21)$$

$$Fe(CN)_6^{3-} + ADF^- \xrightarrow{k_2} Fe(CN)_6^{4-} + ADF^{\bullet} \quad (22)$$

$$H_2Fe(CN)_6^{2-} + ADF^{\bullet} \xrightarrow{k_{-2}} Fe(CN)_6^{3-} + ADF^- + 2H^+ \quad (23)$$

$$Fe(CN)_6^{3-} + HADF^{\bullet+} \xrightarrow{k_3} Fe(CN)_6^{4-} + P + 2H^+ \quad (24)$$

$$Fe(CN)_6^{3-} + ADF^{\bullet} \xrightarrow{k_4} Fe(CN)_6^{4-} + P + H^+ \quad (25)$$

$$HADF^{\bullet+} \overset{K_{HA^{\bullet}}}{\rightleftharpoons} ADF^{\bullet} + H^+ \quad (26)$$

$$r = -\frac{1}{2}\frac{d[Fe(CN)_6^{3-}]}{dt} = \frac{k_1k_3[HADF][Fe(CN)_6^{3-}]^2}{k_3[Fe(CN)_6^{3-}] + k_{-1}[H_2Fe(CN)_6^{2-}]} + \frac{k_2k_4[ADF^-][Fe(CN)_6^{3-}]^2}{k_4[Fe(CN)_6^{3-}] + k_{-2}[H_2Fe(CN)_6^{2-}]} \quad (27)$$

Introduction of initial rates leads to

$$r_0 = \left(k_1\frac{[H^+]}{K_1 + [H^+]} + k_2\frac{K_1}{K_1 + [H^+]}\right)[HADF]_T[Fe(CN)_6^{3-}]_T = k_{obs}[HADF]_T[Fe(CN)_6^{3-}]_T \quad (28)$$

where $[HADF]_T = [HADF] + [ADF^-]$. The observed nondependence of k_{obs} on $[H^+]$ (Table 4, Supporting Information), can be justified assuming that $k_1 = k_2$, that is, the neutral and monoanion HADF forms are of similar reactivity. From the parameters $k_1 = k_2 = 2.18 \pm 0.05$ M^{-1} s^{-1} and $k_{-1}/k_2 = 0.092$ evaluated above, it follows that $k_{-1} = 0.2 \pm 0.03$ M^{-1} s^{-1}. In view that the rate-determining step involves the $HADF^{\bullet+}$ radical species, it can be concluded that $k_3 < k_4$. Bearing in mind the observed experimental features, it stands to reason that $k_1/k_{-1} \approx k_2/k_{-2}$. Although this approach may provide a fair interpretation of the acidity effect, it does not account for the nondependence on temperature, giving way to a somewhat more complex mechanism. Indeed, k_3 cannot be regarded as a slow step, because the hexacyanoferrate (III) oxidation of free radicals normally is diffusion-controlled.[45,46] If one takes for granted that the k_1 and k_{-1} steps and k_2 and k_{-2} are in equilibrium, then the reaction order in the oxidant should be 2 and, therefore, application of the initial rate method would become unfeasible. As occurred with ascorbic acid,[47–50] the probable recombination of the hydroxyfumarate radicals in a diffusion-controlled step, forming HADF and diketosuccinic acid (P), should also be considered. However, this step should be irreversible and very fast, because the HADF and P interaction is thermodynamically unlikely.

Region II. In this region, 1.3 M < $[H^+]$ < 3.0 M, HADF is present only in the neutral form, whereas hexacyanoferrate (III) is split into the nonprotonated and the monoprotonated forms (eq 5). Likewise, hexacyanoferrate (II) is split into the forms represented in eq 7. Given the observed nondependence of the rate constant with ionic strength at 2.0 M HCl, it can be concluded that the rate-determining step involves neutral HADF, the steps involving the radical cation being fast. The rate-determining step of the hexacyanoferrate (III) oxidation of many organic substrates that follow first order in both the oxidant and substrate is the transfer of the first electron from the substrate to the oxidant,[33,37,38] with formation, in this case, of the dihydroxyfumarate free radical; this radical should generate hexacyanoferrate (II) and diketosuccinic acid in the follow-up fast step. In this acidity range the hexacyanoferrate (III)/(II) formal reduction potential rises from 0.688 V (1.0 M HCl) to 0.764 V (3.0 M HCl);[14] therefore, the process described will be even faster when $HFe(CN)_6^{2-}$ is the reactive species. Within this range, the rate constant varies as a function of medium acidity according to

$$k_{obs} = A + B/[H^+] \quad (29)$$

From the data in Table 4, Supporting Information, it follows that $A = (3.44 \pm 0.06) \times 10^{-2}$ and $B = (2.82 \pm 0.01) \times 10^{-3}$ ($r^2 = 0.982$). The mechanism put forward is as follows:

$$Fe(CN)_6^{3-} + HADF \xrightarrow{k_1'} Fe(CN)_6^{4-} + HADF^{\bullet+} \quad (30)$$

$$HFe(CN)_6^{2-} + HADF \xrightarrow{k_2'} HFe(CN)_6^{3-} + HADF^{\bullet+} \quad (31)$$

$$H_2Fe(CN)_6^{2-} + HADF^{\bullet+} \xrightarrow{k'_{-1}} Fe(CN)_6^{3-} + HADF + 2H^+ \quad (32)$$

$$H_3Fe(CN)_6^{-} + HADF^{\bullet+} \xrightarrow{k''_{-1}} HFe(CN)_6^{2-} + HADF + 2H^+ \quad (33)$$

$$Fe(CN)_6^{3-} + HADF^{\bullet+} \xrightarrow{fast} Fe(CN)_6^{4-} + P + 2H^+ \quad (34)$$

$$HFe(CN)_6^{2-} + HADF^{\bullet+} \xrightarrow{fast} HFe(CN)_6^{3-} + P + 2H^+ \quad (35)$$

Bearing in mind that $[Fe(CN)_6^{4-}]_T \approx 0$, application of the steady-state method leads to the initial rate expression:

$$r_0 = \left[k_1' K_5 \cdot \frac{1}{[H^+]} + k_2'\right][HADF]_T[HFe(CN)_6^{2-}] \approx k_{obs}[HADF]_T[Fe(CN)_6^{3-}]_T \quad (36)$$

As shown above, $k_2' > k_1'$; hence, it can be assumed that equilibrium 5 is shifted to the more reactive protonated form. k_{obs} in equation 36 is formally identical to eq 29. Starting from the values for A, B, and K_5 and given the value $[HADF] = 5 \times 10^{-3}$ M, it follows that $k_2' = 6.80 \pm 0.05$ $M^{-1}s^{-1}$ and $k_1' = 0.141 \pm 0.01$ M^{-1} s^{-1}. The k_1' value is 1 order of magnitude lower than the k_1 evaluated in region I ($k_1 = 2.18 \pm 0.05$ M^{-1} s^{-1}), which supports the idea that the deprotonated hexacyanoferrate (III) amount in region II is less.

Region III: $[H^+]$ > 3.0 M. In this region, hexacyanoferrate (III) is split into the forms shown in eq 4, whereas hexacyanoferrate (II) is split into the monoanion and the

neutral forms shown in eq 6. The sharp increase in rate with medium acidity (Figure 6) denotes a complex relation in the form

$$r = [HFe(CN)_6^{2-}]_T \cdot [HADF]_T f([H^+]) \quad (37)$$

where $[HFe(CN)_6^2]_T = [HFe(CN)_6^{2-}] + [H_2 Fe(CN)_6^-]$. At HCl = 6.0 M, the reduction potential of the hexacyanoferrate (III/II) couple, E^0, rises with medium acidity up to $E^0 = 0.858$ V.[14] However, the observed sharp increase in rate can be rationalized only if another rather more reactive species, such as H_2ADF^+, is generated in equilibrium with the neutral form.

$$H_2ADF^+ \overset{K_{HA}}{\rightleftharpoons} HADF + H^+ \quad (38)$$

with $[HADF]_T = [HADF] + [H_2ADF^+]$.

Combination of eqs 4, 6, and 37 leads to the following mechanism:

$$HFe(CN)_6^{2-} + HADF \xrightarrow{k_2'} HFe(CN)_6^{3-} + HADF^{\bullet+} \quad (39)$$

$$H_2Fe(CN)_6^{2-} + HADF \xrightarrow{k_2''} H_2Fe(CN)_6^{-} + HADF^{\bullet+} \quad (40)$$

$$HFe(CN)_6^{2-} + H_2ADF^+ \xrightarrow{k_3'} HFe(CN)_6^{3-} + HADF + H^+ \quad (41)$$

$$H_2Fe(CN)_6^{-} + H_2ADF^+ \xrightarrow{k_3''} H_2Fe(CN)_6^{-} + HADF^{\bullet+} + H^+ \quad (42)$$

$$H_3Fe(CN)_6^{-} + HADF^{\bullet+} \xrightarrow{\text{fast}} HFe(CN)_6^{2-} + HADF + 2H^+ \quad (43)$$

$$H_4Fe(CN)_6 + HADF^{\bullet+} \xrightarrow{\text{fast}} H_2Fe(CN)_6^{-} + HADF + 2H^+ \quad (44)$$

which leads to the initial rate equation

$$r_0 = \frac{k_2' K_4 K_{HA} + (k_2'' K_{HA} + k_3' K_4)[H^+] + k_3''[H^+]^2}{K_4 K_{HA} + (K_4 + K_{HA})[H^+]} \cdot [HFe(CN)_6^{2-}]_T [HADF]_T \quad (45)$$

Because of the large number of parameters to be determined, the experimental data-pairs fit only roughly to this equation. A convincing interpretation can be provided if $k_3'' > k_3'$, $k_2'' > k_2'$, $k_3' > k_2'$, and $k_3'' > k_2''$; on the other hand, the $K_4 = 1698$ and K_{HA} values are expected to be only approximated, since the two equilibria (eqs 4 and 38) come about within the same acidity range.

Conclusions

The hexacyanoferrate (III) oxidation of HADF in acidic media is a rather complex reaction prone to three different reaction schemes depending on the medium acidity. Involvement of radical species in all three mechanisms has been unambiguously proved. The role played by the dihydroxyfumarate radical in the rate-determining step depends on the extent of protonation of both reactants and reaction products. Unlike other endiol species, a specific catalytic effect by binding of alkali metal ions to the oxidant was not observed.

Acknowledgment. The financial support by Ministerio de Educación y Ciencia, Project CTQ2006-14734/BQU, cofinanced by FEDER, and Junta de Castilla y León, Project BU 001A-06, is gratefully acknowledged.

Supporting Information Available: Tables showing the initial rate as a function of both initial $Fe(CN)_6^{4-}$ and initial oxidant concentrations, as well as k_{obs} values as a function of both solvent permittivity and medium acidity. This material is available free of charge via the Internet at http://pubs.acs.org.

References and Notes

(1) Hough, L.; Jones, J. K. N. *Nature* **1951**, *167*, 180.

(2) Sychev, A.; Duka, G. G. *Sadovod. Vinograd. Vinodel. Mold.* **1985**, *12*, 34.

(3) Nelson Research and Development Co. JPN. Tokkio Koho, 8105, 971 (Cl. G02C7/04), 07 Feb. (1981), VS. Appl. M666,067, 11 Nar (1976); pp 10.

(4) Hubert, V. Ger. Offen. DE, 3, 030, 476, (Cl. A01N59/00) 19 Mar (1981), Brit. Appl. 79/30, 588, 04 Sep (1979); pp 14.

(5) Fredk, R. U.S. US 4, 526, 701 (Cl. 252−113; C11D9/00) 02 Jul (1985), Appl. 297, 588, 31 August. (1981); pp 6.

(6) D'Amico, A.; Chiesa, F.; Montaldi, D.; Quarenghi, F. *Bull. Soc. Chim. Fr.* **1962**, *101*, 903.

(7) Gupta, M. P. *Capad. J. Chem.* **1955**, *33*, 450.

(8) Hay, R. W.; Harvie, S. J. *Aust. J. Chem.* **1965**, *18*, 1197.

(9) Fleury, M. *Comptes Rendus* **1961**, *252*, 1931.

(10) Sazou, D.; Karabinas, P.; Jannakoudakis, D. *J. Electroanal. Chem.* **1984**, *176*, 225.

(11) Sochay, P.; Fleury, D.; Fleury, M. *Acad. Sci. Paris, Ser. C.* **1967**, *264*, 2130.

(12) Fleury, D. *Bull. Soc. Chim. Fr.* **1970**, *1*, 370.

(13) Hitoshi, O.; Michiaki, T.; Tai, T. *Agric. Biol. Chem.* **1981**, *45*, 1011.

(14) Leal, J. M.; García, B.; Domingo, P. L. *Coord. Chem. Rev.* **1998**, *173*, 79.

(15) Pushparaj, F. J. M.; Kannan, S.; Vikram, L.; Kumar, L. S.; Rangappa, K. S. J. *J. Phys. Org. Chem.* **2005**, *18*, 1042.

(16) Tandon, P. K.; Sing, A. K.; Baboo, R.; Kumar, S.; Saxena, A. K.; Singh, M. P. *Oxid. Commun.* **2005**, *28*, 611.

(17) Goel, A.; Chauhan, M.; Shailja, J. *Asian J. Chem.* **2006**, *18*, 1116.

(18) Tandon, P. K.; Kumar, S.; Srivastava, M.; Khanam, S. Z.; Singh, S. B. *J. Mol. Catal. A: Chem.* **2007**, *26*, 282.

(19) Poblete, F. J.; Mucientes, A. E.; Villarreal, S.; Santiago, F.; Cabanas, B.; Gabaldon, R. E. *J. Phys. Org. Chem.* **2006**, *19*, 597.

(20) Behari, V.; Behari, K. *Transition Met. Chem.* **2007**, *32*, 262.

(21) Nelson, E. P.; Phengsy, P. P. *Int. J. Chem. Kinet.* **2000**, *32*, 760.

(22) Mucientes, A. E.; Santiago, F.; Almena, M. C.; Poblete, F. J.; Rodríguez- Cervantes, A. M. *Int. J. Chem. Kinet.* **2002**, *34*, 421.

(23) Farokhi, S. A.; Nandibewoor, S. T. *Tetrahedron* **2003**, *59*, 7595.

(24) Mucientes, A. E.; Gabaldon, R. E.; Poblete, F. J.; Villarreal, S. *J. Phys. Org. Chem.* **2004**, *17*, 236.

(25) El-Aila, H. Y. J. *J. Dispersion Sci. Technol.* **2004**, *25*, 157.

(26) Franke, W.; Brathun, G. *Liebigs Ann.* **1931**, *487*, 1.

(27) Steinberg, S.; Westheimer, F. H. *J. Am. Chem. Soc.* **1951**, *73*, 429.

(28) Hrusák, J.; McGibbon, G. A.; Schwarz, H.; Terlouw, J. K. *Int. J. Mass Spectrom. Ion Processes* **1997**, *160*, 117.

(29) Fleury, M. *Comptes Rendus* **1965**, *260*, 5563.

(30) Domingo, P. L.; García, B.; Leal, J. M. *Can. J. Chem.* **1990**, *68*, 228.

(31) Domingo, P. L.; García, B.; Leal, J. M. *Can. J. Chem.* **1987**, *65*, 583.

(32) Abe, Y.; Dohmaru, T.; Horii, H.; Taniguchi, S. *Can. J. Chem.* **1985**, *63*, 1105.

(33) Merohtra, V. S.; Agrawal, M. C.; Mushram, S. P. *J. Phys. Chem.* **1969**, *73*, 1196.

(34) Martínez, P.; Uribe, D. *An. Quim., Ser. A* **1980**, *76*, 201.

(35) Roy, P. R.; Saha, M. S.; Okajima, T.; Ohsaka, T. *Electrochim. Acta* **2005**, *51*, 4447.

(36) Pelizzetti, E.; Mentasti, E.; Pramauro, E. *Inorg. Chem.* **1978**, *17*, 1181.

(37) Ferrari, L.; Alonso, A. *An. Quim., Ser. A* **1983**, *79*, 531.

(38) Acharya, S.; Neogi, G.; Panda, R. K. *Z. Phys. Chem. Leipzig* **1986**, *267*, 1189.

(39) Sazou, D.; Karabinas, P.; Jannakoudakis, D. *J. Electroanal. Chem.* **1985**, *185*, 305.
(40) Leal, J. M.; Domingo, P. L.; García, B.; Ibeas, S. *J. Chem. Soc., Faraday Trans.* **1993**, *89*, 3571.
(41) Sychev, A.; Duka, G. G. *Zh. Fiz. Khim.* **1983**, *57*, 1938.
(42) Sychev, A.; Duka, G. G. *Zh. Fiz. Khim.* **1979**, *53*, 510.
(43) Espenson, J. H. *Chemical Kinetics and Reactions Mechanisms*, 2nd ed.; McGraw-Hill: New York, 1995.
(44) Laidler, K. J. *Chemical Kinetics*; McGraw-Hill: New York, 1987.
(45) Steenken, S.; Neta, P. *J. Am. Chem. Soc.* **1982**, *104*, 1244.
(46) Steenken, S.; Buschek, J.; McClelland, R. A. *J. Am. Chem. Soc.* **1986**, *108*, 2808.
(47) Hughes, G.; Willis, C. *Discuss. Faraday Soc.* **1963**, *36*, 223.
(48) Yamazaki, I.; Mason, H. S.; Piette, L. *J. Biol. Chem.* **1960**, *235*, 2444.
(49) Yamazaki, I.; Piette, L. *Biochim. Biophys. Acta* **1961**, *50*, 62.
(50) Bielski, B. H. J.; Comstock, D. A.; Bowen, R. A. *J. Am. Chem. Soc.* **1971**, *93*, 5624.

JP800208S